
Ray-reflectivity method for the P - S_V case: Basic numerical results

P.F. Daley

ABSTRACT

In an earlier report the theory for the implementation of the ray-reflectivity method has been presented. The use of this method for realistic geological situations might be counterproductive, as a demonstration of many of the basic developments could be lost. Possibly the most interesting of these is what has been termed the *tuning* of the thin layer using different variations of input parameters. As a result only a simple model consisting of a layer over a half space is considered. These two media are separated by a thin transition layer in which the elastic parameters can be chosen for it to be either a low or high velocity channel. The main objectives of this report are to present the reflected *PP* and *PS* reflectivities from the top of the thin layered zone. The reflectivities are dependent on, apart from the elastic parameters of the layer, thin layer and half space, angle of the incident wave type, thickness of the thin layer and frequency. The most efficient manner of doing this is with 3D plots; reflectivity amplitude versus incident angle and frequency being one possibility. Additionally, some simple reflection synthetic seismograms will be shown to indicate the change in the seismic traces as a result of changes in, say, the predominant frequency of the source wavelet.

DISCUSSION OF METHODS AND MODELS

The ray-reflectivity approach to computing synthetic seismograms in a plane parallel medium where the interfaces between *thick* layers may be a thin layered is a hybrid method combining asymptotic ray (zero order geometrical optics) and propagator matrix theories. It allows a flexibility that neither pure ray methods nor matrix or reflectivity methods alone offer, while still maintaining reasonable processing speed. It is moderately specific in the types of geometries it can efficiently deal with, these geometry types being geological structures often associated with hydrocarbon deposits. A fairly complete coverage of this topic is given in an associated report that contains a detailed derivation of this methodology for the $P-S_V$ problem (Daley, 2006) where numerous references related to the theory of this topic may be found. For completeness a brief description will be presented here. The related S_H case has been dealt in a series of papers over the past 25 years (Daley and Hron, 1982, 1990, 1992).

In a radially symmetric plane parallel isotropic homogenous medium composed of *thick* layers separated by thin layered transition zones the general form of the horizontal and vertical particle displacement vector components, for some specified ray, recorded at the earth's surface, due to a surface source is given by

$$\mathbf{u}(r, z, \omega) = [u, w]^T = \frac{f(\omega) \left[\sum_{j=1}^{2N-1} R_{mn}^{(j)}(p_0, \omega) \right]}{L} \left[S_c^{(V)}, S_c^{(H)} \right]^T. \quad (1)$$

with the superscript "T" indicating transpose.

In the above a ray with segments is assumed, so that it will have $2N-1$ interactions with a boundary between in the thick layers, which modify the amplitude through the reflectivities and transmittivities, $R_{mn}^{(j)}(p_0, \omega)$ in the summation term. These coefficients are functions of the elastic parameters in incident medium (m), the medium of reflection or transmission (n), and the related thin layered zone as well as the ray parameter, p_0 , and frequency, ω . The source and receiver, which are both located on the surface, are not included in this count, the energy at the receiver being partitioned by the surface conversion coefficients, $S_c^{(V)}$ and $S_c^{(H)}$, which may be the result of P or S_v ray incidence. The geometrical spreading along the ray, L is computed only in the thick layers, and using two point ray tracing, the ray parameter, p_0 , is also determined using the thick layers. However, in the computer code for the production of synthetics, some adjustment to p_0 is made to account for the thin layered zones, especially at far offsets. As computations must be done in the frequency domain, a bandlimited source wavelet, $f(t)$, with Fourier transform, $f(\omega)$, is assumed.

NUMERICAL RESULTS

The first matter that will be given consideration is the incident angle – frequency – thin layer thickness relationship contained within the reflectivities and transmittivities. The model chosen for this is a 100m high velocity thin layer between two half spaces with different velocities. The P - wave velocities in the thin layer and half spaces were chosen after the choice of the thin layer and frequency range of 0–100Hz was made. As a consequence the velocities may appear unphysical but are justified as the resultant figures display the effect of introducing the thin high velocity zone without being masked by rapid oscillations. Also, the thicknesses and velocities can be simultaneously scaled. The shear velocities, β in all layers were chosen such that $\beta = \alpha/\sqrt{3}$. The densities, ρ_j , used are, in descending order from surface layer to half space, 2.0, 2.6 2.1 gm/cm^3 .

The P velocity depth schematic is given in Figure (1). The coefficients chosen are fairly standard as P - wave incidence from the upper half space and P - wave and S_v - wave reflections in the first layer are plotted in Figures (4) and (5). These coefficients are denoted P_0P_0 and P_0S_0 in the figures mentioned. In both figures the bottom plot shows the reflectivity over the range of frequencies 0–10Hz. This was done so that they could be compared to the case without a thin layer zone, which they appear to emulate fairly accurately. This is expected in this frequency range, as a seismic wavelet in this frequency range would not be able to resolve the thin layer since the predominant wavelength would be of the order of 500m or more.

The top plot in both Figures (2) and (3) show the amplitude of the P_0P_0 and P_0S_0 reflectivities for the frequency range of 0–100Hz and an incident angle range of 0 – 90 degrees. The “tuning” effect of the thin layer in the frequency dimension can be clearly seen in both figures. At angles near normal incidence a local maximum of the P_0P_0 reflectivity corresponds to a local minimum of the P_0S_0 reflectivity. The splitting of the reflected arrivals from the top and bottom of the “thin” layer is best seen in the P_0P_0 reflectivity, starting about 60Hz corresponding to a predominant wavelength of the order of the thickness of the *thin* layer”. This effect is less visible in the P_0S_0 reflectivity.

To show the effect on the reflectivities of replacing the thin high velocity with a low velocity layer of the same thickness the amplitudes of the P_0P_0 and P_0S_0 for this case are shown in Figure (4). The velocity depth structure is shown as the dashed portion of Figure (3). As in the previous figures the shear wave velocities are given by the relation $\beta = \alpha/\sqrt{3}$ and the density of the thin layer used is 1.8 gm/cm^3 .

Synthetic traces will be computed for a modified version of the above model where the single “thin” layer will still be the only indication of the reflectivity method. A thick layer will replace the upper half space where a source and receivers will be located. The source wavelet used is the bandlimited Gabor wavelet defined as

$$f(t) = \sin \omega_0 t \exp \left[- \left(\frac{\omega_0 t}{\gamma} \right)^2 \right] = \text{Im} \left[e^{i\omega_0 t} \right] \exp \left[- \left(\frac{\omega_0 t}{\gamma} \right)^2 \right], \quad (0 \leq t \leq t_h). \quad (2)$$

The predominant circular frequency of the pulse is $\omega_0 = 2\pi f_0$, f_0 the predominant frequency. A damping factor γ that controls the size of the side lobes of the pulse in the time domain is usually taken to be 4.0. The quantity t_h is the approximate half-width of the source pulse given as $t_h \approx \gamma/2f_0$. Synthetic sections will be computed for this very simple model for two values of f_0 ; 30Hz and 90Hz. In the synthetic traces shown in Figures (5) and (6) the upper layer is 1000m thick, and the thin layer vertical dimension is changed to 50m. The velocities used are for the high velocity case shown in Figure (1). Defining a wavelength with respect to the velocity in the upper layer and the predominant frequencies of the source pulses used has a wavelength defined as 167m and 56m, respectively.

The two sets of synthetic traces computed are for the vertical and horizontal components of particle displacement and are shown for the two frequencies of the source wavelet described above. Only the reflected *PP* and *PS* arrivals (indicated on the figures) are shown in the synthetics. These arrivals contain the reflected arrivals from the top of the thin layer together with all inter-bed multiples and conversions, i.e., the total wave field response from the thin layer.

This total wave field response is more apparent in Figure (7) where the low velocity is used in the thin layer and just the vertical components of particle displacement are

displayed. Again only the PP and PS rays are generated in the thick surface layer and the predominant frequencies of 30 and 90 Hz are used in the source wavelet. The inter-bed reverberations from the thin layer consisting of multiples and converted phases comprise the additional arrivals.

A question which might be asked is “Why not just treat the thin layer as a thick layer and generate rays to produce a zero order asymptotic ray theory synthetic that includes the inter-bed multiples and conversions?” If a layer is truly *thin*, then asymptotic ray theory or any high frequency approximation solution is suspect in this case. In addition, if the moduli of the P_0P_0 and P_0S_0 reflectivities shown in Figures (4) - (6) are an indication, the thin layers serve as frequency filters, removing predictable frequencies from the seismic response. This effect is often referred to as “tuning”, possibly a misnomer.

As a final set of examples a classic model presented in Fuchs and Müller (1971) is considered. This model consists of a background model with constant P and S_v velocities and densities as shown in Figure (8). Embedded in this model are two coal seams of 2m thickness at depths of 200m and 250m. All model parameters are given in Figure (8) and its caption. In this case vertical and horizontal components of particle displacement recorded at the surface due to point sources of both P and S_v waves. All rays with a maximum of 8 segments are used. Up to 2 conversions per ray are also allowed and included in the synthetics, provided they arrive within the specified time window. A Gabor wavelet with a predominant frequency of 60 Hz and a damping factor of $\gamma = 4.0$ is used. The resulting synthetics are shown in Figures (9) and 10.

CONCLUSIONS

Utilizing what have been presumed to be some of the best qualities of both asymptotic ray theory and the reflectivity method some simple results utilizing this hybrid method have been presented. The method is employed to consider the seismic response from a plane parallel layered isotropic structure composed of thick layers, where asymptotic ray methods are used, separated by thin layered zones, where the validity of asymptotic ray theory is questionable and reflectivity (matrix) methods are used. The fact that the computation time is increased as the computation of synthetic sections must be done in the frequency domain is somewhat compensated for when models with large number of layers are considered as the number of rays that are required to be used can be significantly reduced.

The numerical examples presented here are not representative of the numerous applications of this method. It incorporates the flexibility of asymptotic ray theory, including the ability to identify individual “thick” layered arrivals, with accuracy comparable to the reflectivity method without the need for numerical integration. As the reflectivity method produces the total wave field response, arrival identification is difficult without resorting to producing travel time tables usually by a two point ray tracing algorithm which is a significant part of the cost of using the ray reflectivity method

ACKNOWLEDGEMENTS

The author acknowledges the support of CREWES and its sponsors.

REFERENCES

- Daley, P.F., 2006, Ray-reflectivity method: Part 1 theory for the $P - S_v$ case: CREWES Report, **18** (this volume).
- Daley, P.F. and Hron, F., 1992, Application of the ray-reflectivity method to multilayered thin bed structures, *Bull. Seism. Soc. Am.*, **82**, 914-933.
- Daley, P.F. and Hron, F., 1990, The ray-reflectivity method with critically refracted waves, *Bull. Seism. Soc. Am.*, **80**, 995-1013.
- Daley, P.F. and Hron, F., 1982, Ray-reflectivity method for SH waves in stacks of thick and thin layers, *Geophys. J. Roy. astr. Soc.*, **69**, 527-536.
- Fuchs, K. and Müller, G., 1971, Computation of synthetic seismograms with the reflectivity method and comparison with observations, *Geophys. J. Roy. astr. Soc.*, **23**, 417-433.

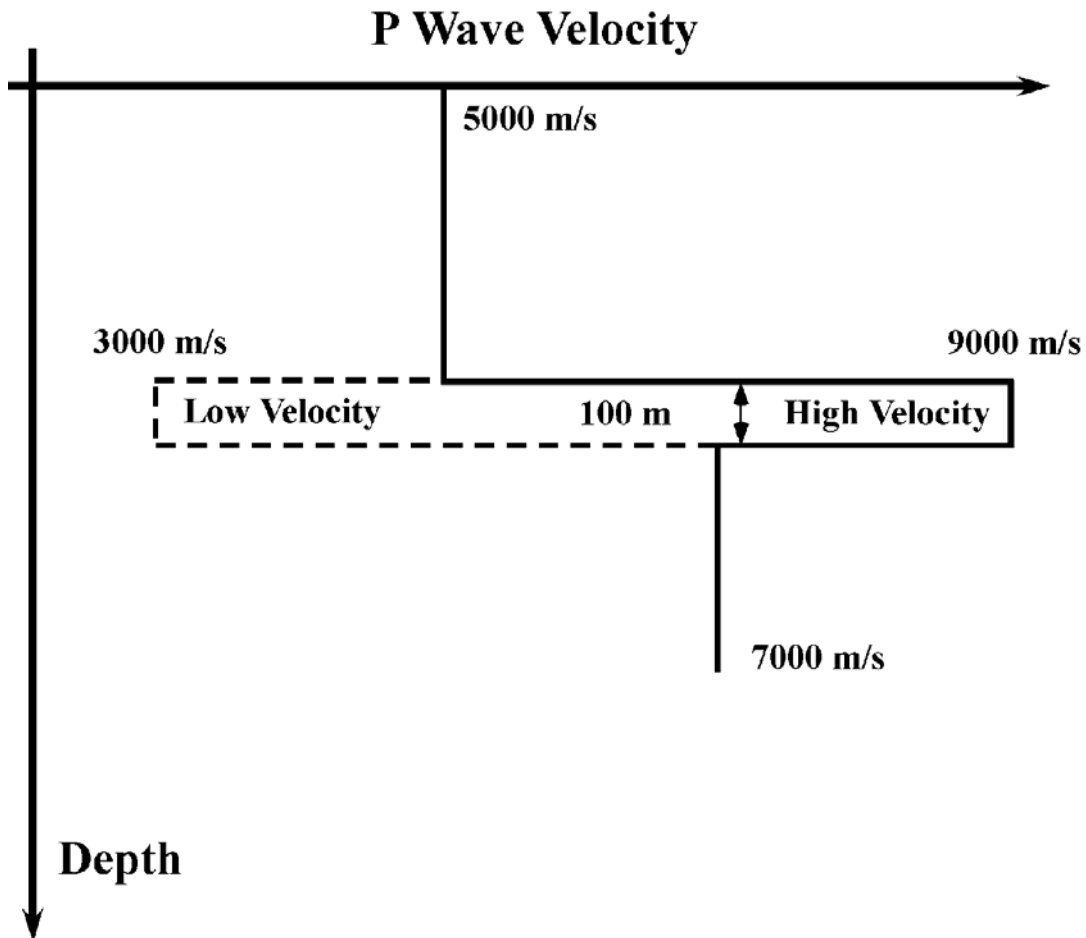


FIG. 1. Compressional, P - wave velocity depth diagram for both a 100m thin high and low velocity layer between a surface layer and halfspace of differing velocities. The shear wave velocities, β_m , are obtained from the P - wave velocities using the relation $\beta_m = \alpha_m / \sqrt{3}$ and the densities, ρ_m are 2.2, 2.6(1.8), 2.1 gm/cm^3 .

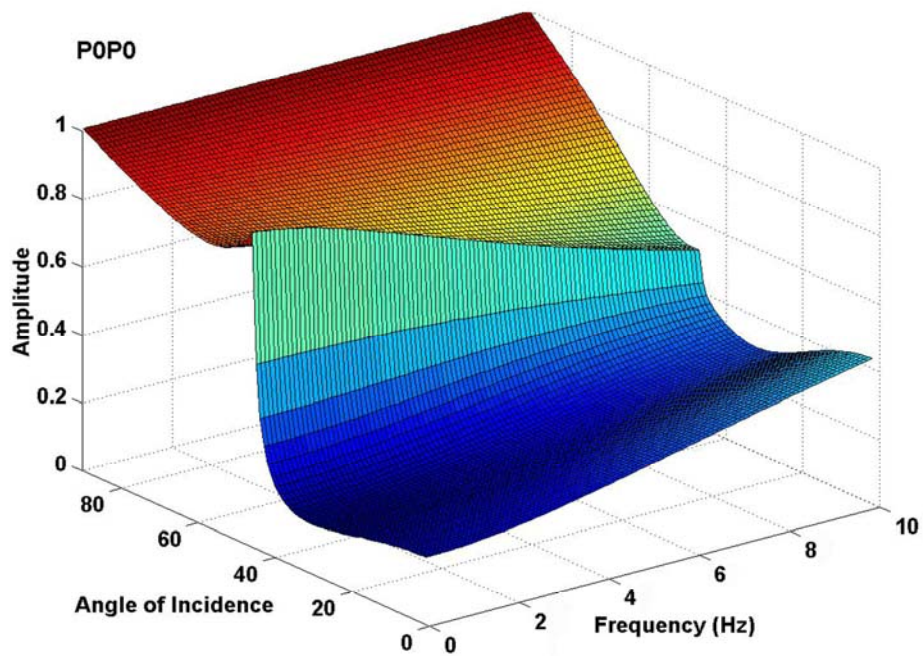
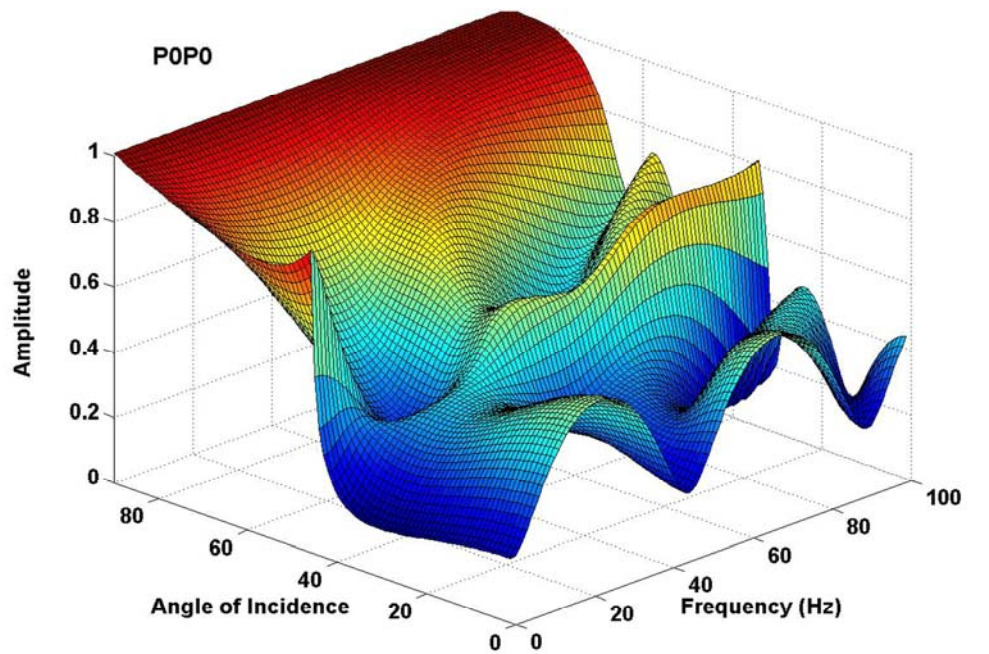


FIG. 2. The amplitude of the complex reflectivity P_0P_0 plotted versus incident angle and frequency. On the lower plot a frequency range of 0–10 Hz is displayed to indicate that at these frequencies the P_0P_0 reflectivity is similar the reflection coefficient at a solid/solid boundary.

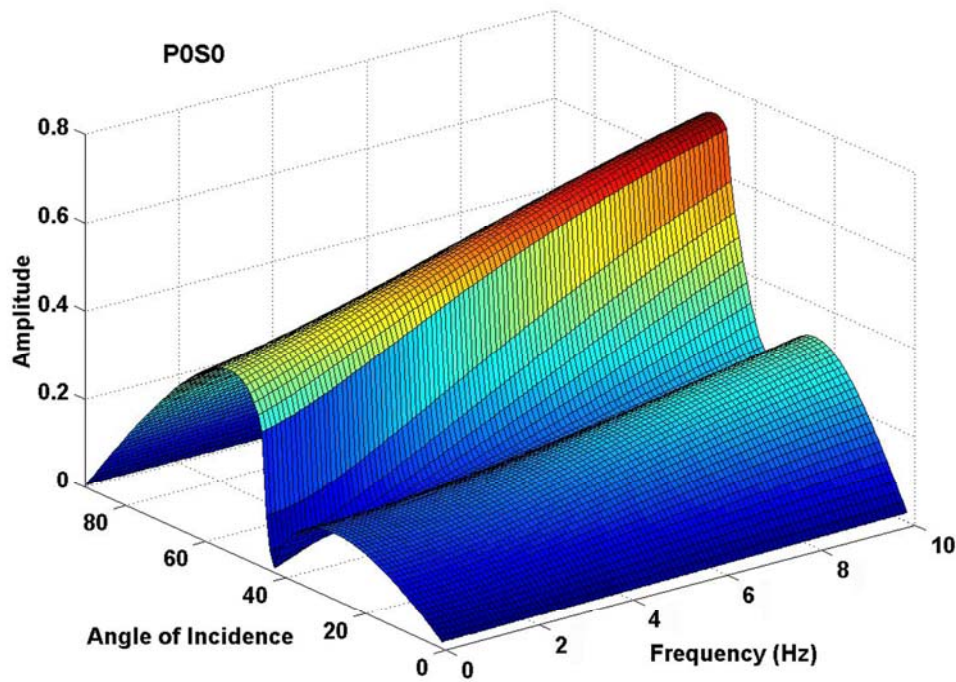
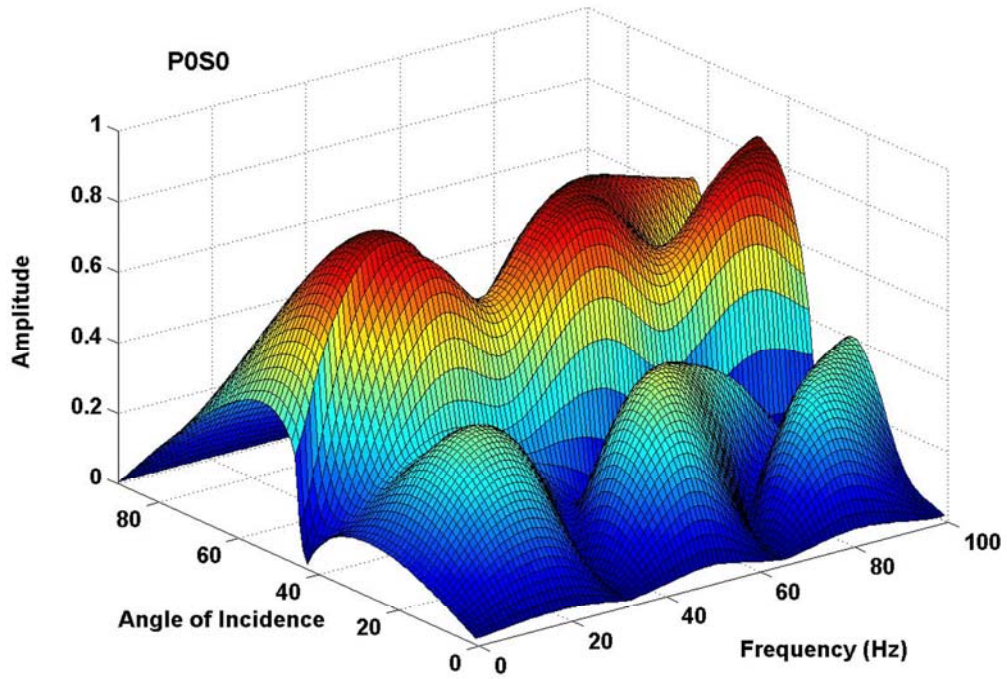


FIG. 3. The amplitude of the complex reflectivity P_0S_0 plotted versus incident angle and frequency. On the lower plot a frequency range of 0–10 Hz is displayed to indicate that at these frequencies the P_0S_0 reflectivity is similar the reflection coefficient at a solid/solid boundary.

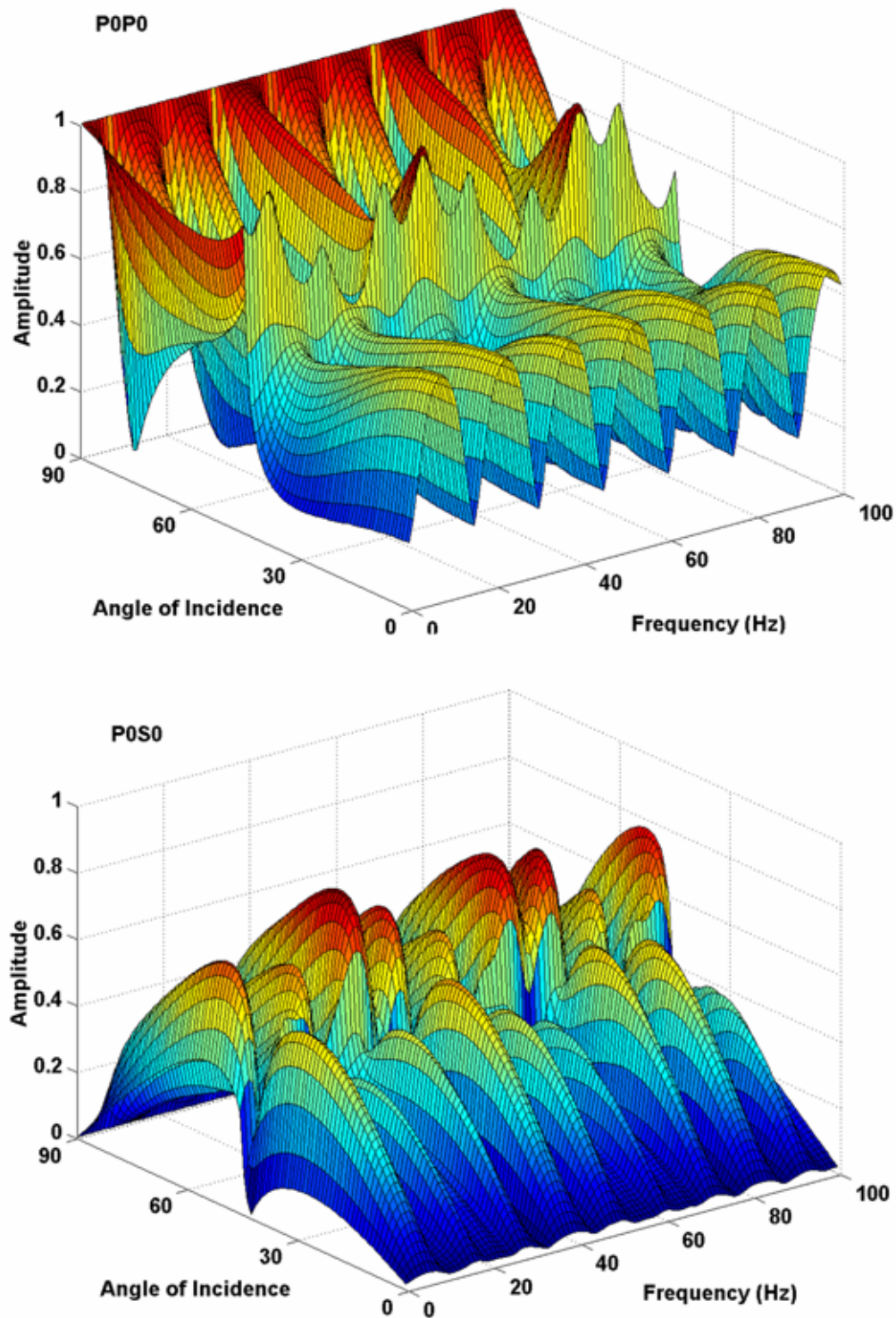


FIG. 4. The amplitudes of the complex P_0P_0 and P_0S_0 reflectivities plotted versus incident angle and frequency. These plots assume a low velocity thin layer as shown in the dashed thin layered portion of Figure 3.

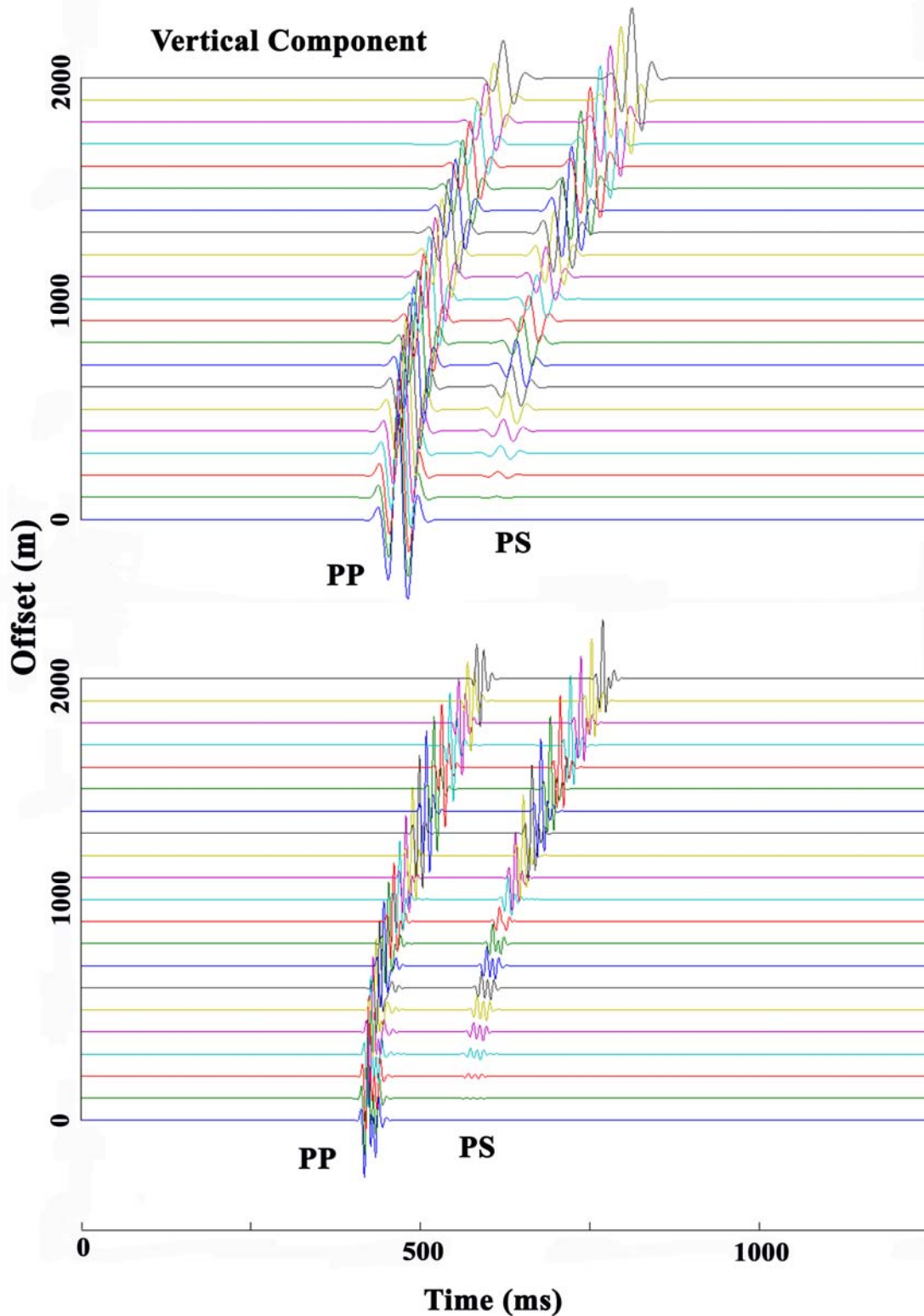


FIG. 5. Vertical component of particle displacement for the 50m thin layer model text. The upper synthetic is for a predominant source frequency of 30Hz while the lower uses a predominant frequency of 90Hz .

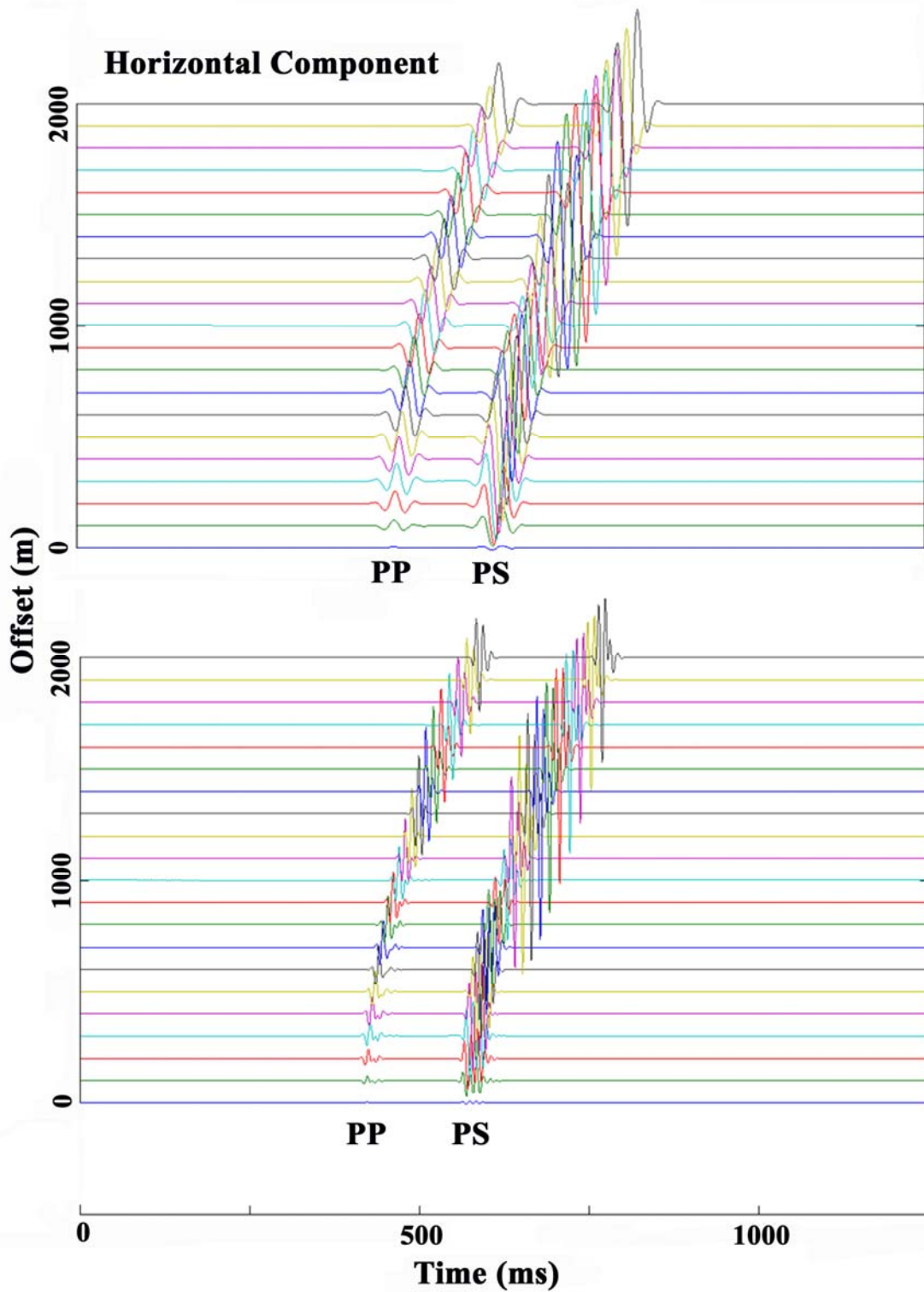


FIG. 6. Horizontal component of particle displacement for the 50m thin layer model text. The upper synthetic is for a predominant source frequency of 30Hz , while the lower uses a predominant frequency of 90Hz .

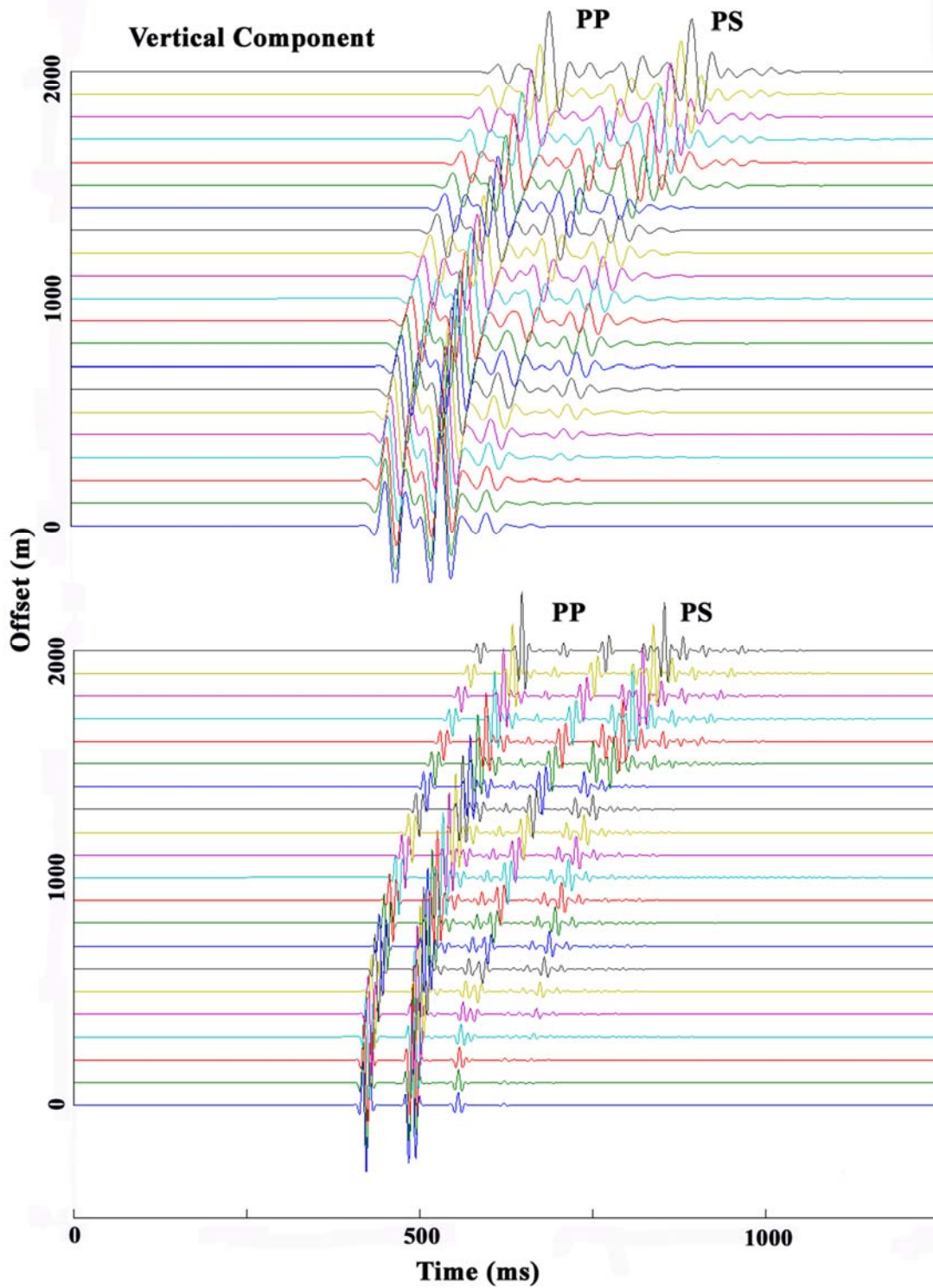


FIG. 7. The vertical components of particle displacements for a 30 Hz (top) and 90 Hz (bottom) Gabor wavelet. In this figure the low rather than the high velocity thin layer is used in synthetic trace production.

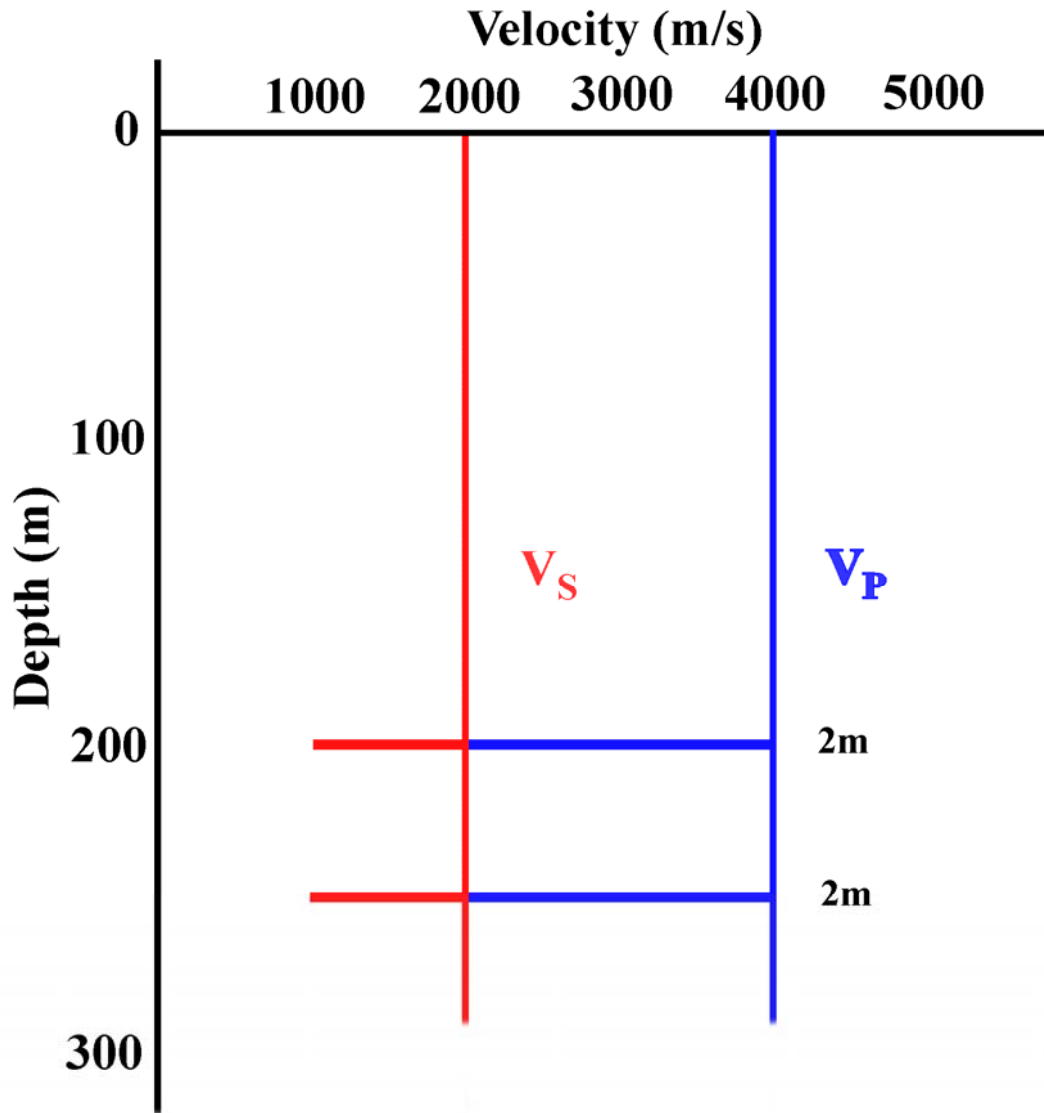


FIG. 8. Velocity – depth schematic for the Fuchs - Muller model. The P and S_v velocities for the background medium are 4000m/s and 2000m/s respectively while the density is 2.0 gm/cm^3 . In the two thin 2m coal seams these values are 2000m/s , 1000m/s and 1.8 gm/cm^3 . In the synthetics a large number of rays are shot, not just the P down - P up and P down - S_v up rays that appear in other synthetics in this report.

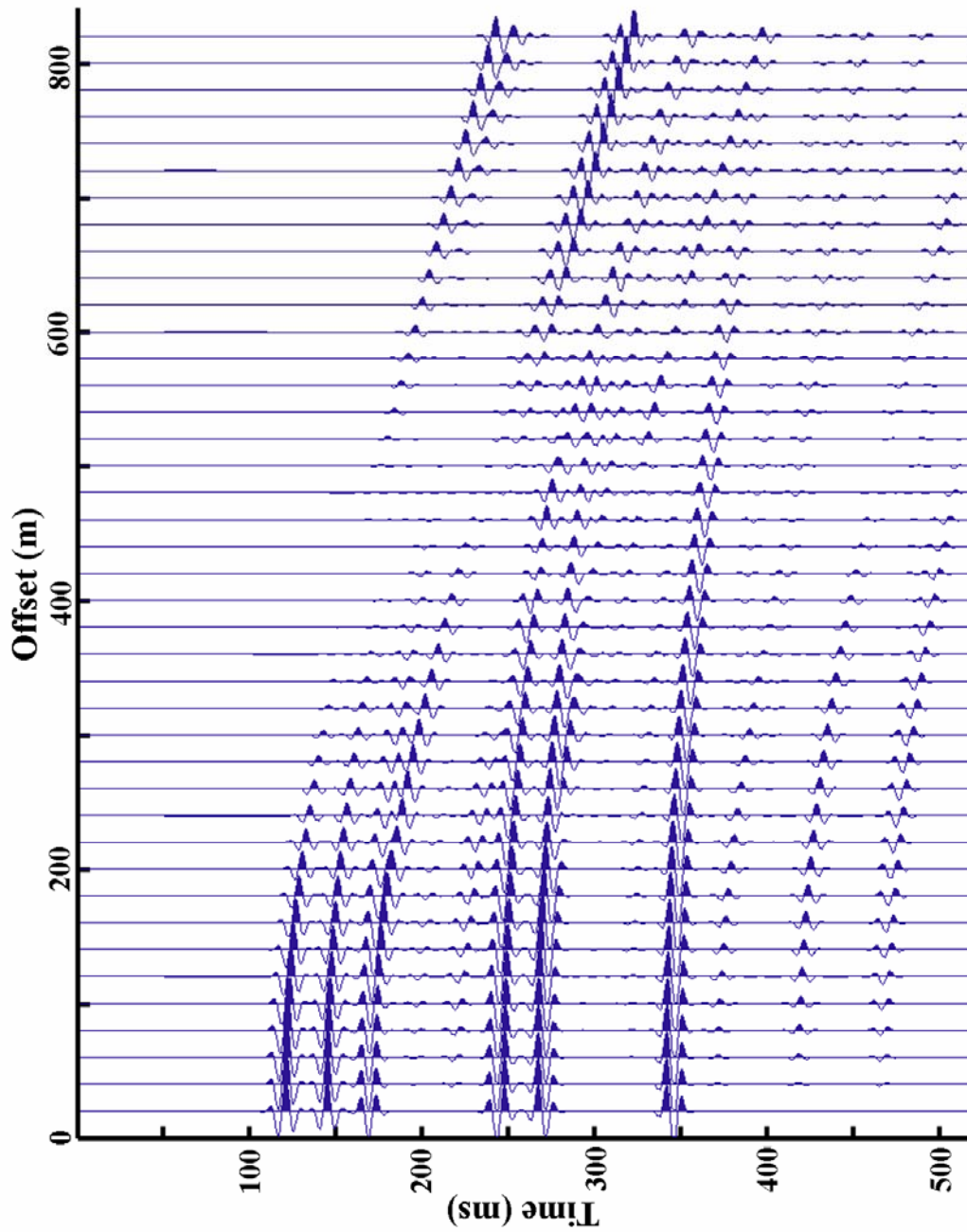


FIG. 9. Vertical component of coal seam model with no scaling. Multiples and converted phases are included.

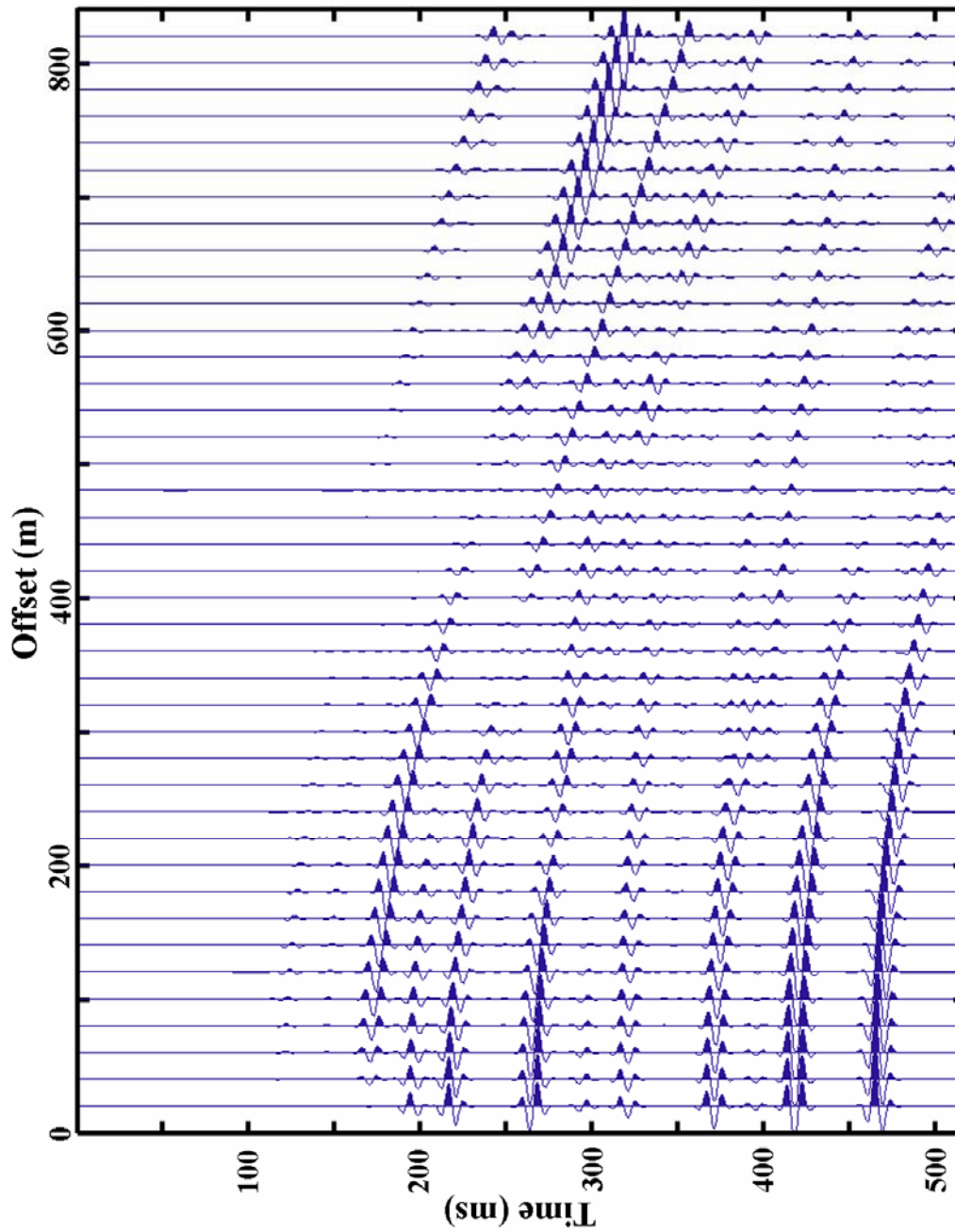


FIG. 10. Horizontal component of coal seam model with no scaling. Multiples and converted phases are included.